HHS Public Access

Author manuscript

Semin Oncol. Author manuscript; available in PMC 2018 October 10.

Published in final edited form as:

Semin Oncol. 2017 June ; 44(3): 204–217. doi:10.1053/j.seminoncol.2017.10.002.

Mitochondrial and glycolytic metabolic compartmentalization in Diffuse Large B Cell Lymphoma

Mahasweta Gooptu[1], **Diana Whitaker-Menezes**[2], **John Sprandio**[3], **Marina Domingo-Vidal**[2], **Zhao Lin**[2], **Guldeep Uppal**[4], **Jerald Gong**[4], **Roberto Fratamico**[2], **Benjamin Leiby**[5], **Alina Dulau-Florea**[6], **Jaime Caro**[7], and **Ubaldo Martinez-Outschoorn**[2,*]

[1]Department of Medical Oncology, Dana Farber Cancer Institute, Harvard University Medical School, Boston, MA

[2]Department of Medical Oncology, Sidney Kimmel Cancer Center, Thomas Jefferson University, Philadelphia, PA

[3]Department of Medical Oncology Chester County Hospital, West Chester, PA

[4]Department of Pathology, Anatomy and Cell Biology, Sidney Kimmel Cancer Center, Thomas Jefferson University, Philadelphia, PA

[5]Department of Clinical Pharmacology, Division of Biostatistics, Thomas Jefferson University, Philadelphia, PA, USA

[6]Department of Laboratory Medicine, Hematology, National Institutes of Health, Bethesda, MD

[7]Department of Medicine, Cardeza Foundation for Hematological Research, Thomas Jefferson University, Philadelphia, PA USA

Abstract

Metabolic heterogeneity between neoplastic cells and surrounding stroma has been described in several epithelial malignancies; however, the metabolic phenotypes of neoplastic lymphocytes and neighboring stroma in diffuse large B-cell lymphoma (DLBCL) is unknown. We investigated the metabolic phenotypes of human DLBCL tumors by using immunohistochemical markers of glycolytic and mitochondrial oxidative phosphorylation (OXPHOS) metabolism. The lactate importer MCT4 is a marker of glycolysis, whereas the lactate importer MCT1 and TOMM20 are markers of OXPHOS metabolism. Staining patterns were assessed in 33 DLBCL samples as well as 18 control samples (non-neoplastic lymph nodes). TOMM20 and MCT1 were highly expressed in neoplastic lymphocytes, indicating an OXPHOS phenotype, whereas non-neoplastic lymphocytes in the control samples did not express these markers. Stromal cells in DLBCL samples strongly expressed MCT4, displaying a glycolytic phenotype, a feature not seen in stromal elements of non-neoplastic lymphatic tissue. Furthermore, the differential expression of

*Corresponding Author: Ubaldo Martinez Outschoorn, MD, Department of Medical Oncology Sidney Kimmel Cancer Center , 233 S. 10th Street Suite 909 Philadelphia, PA, 19107, Phone: 2159558874, ubaldo.martinez-outschoorn@jefferson.edu.

The authors disclose no potential conflicts of interest

lactate exporters (MCT4) on tumor associated stroma and lactate importers (MCT1) on neoplastic lymphocytes support the hypothesis that neoplastic cells are metabolically linked to the stroma likely via mutually beneficial reprogramming. MCT4 is a marker of tumor-associated stroma in neoplastic tissue. Our findings suggest that disruption of neoplastic-stromal cell metabolic heterogeneity including MCT1 and MCT4 blockade should b studied to determine if it could represent a novel treatment target in DLBCL.

Keywords

monocarboxylate transporter; oxidative phosphorylation; glycolysis; tumor-microenvironment

INTRODUCTION

The characterization of metabolic profiles of neoplastic cells and their surrounding stromal cells may help us understand how tumors that have high metabolic requirements meet their significant needs. Tumor associated stromal cells include fibroblasts, antigen presenting cells- (APCs), plasma cells, neutrophils and macrophages. Most human cells utilize glucose as their primary substrate and metabolize it to produce energy in the form of ATP as well as to generate intermediates for building biomolecules [1]. Typically, glucose enters the cell and undergoes numerous enzymatic reactions to generate pyruvate. Pyruvate may then follow one of two paths; it may be reductively metabolized to form lactate and released from cells via monocarboxylate transporter 4 (MCT4), a process known as glycolysis. Alternatively, pyruvate is converted to acetyl CoA and is metabolized in mitochondria through the tricarboxylic acid (TCA) cycle and oxidative phosphorylation (OXPHOS) to generate ATP. Glycolysis, or the conversion of glucose into lactate through pyruvate, is much less energetically efficient than OXPHOS since it generates 2 molecules of ATP per molecule of glucose compared to 36 molecules of ATP with OXPHOS [2]. However, glycolysis generates ATP at a faster rate than OXPHOS [2]. This trade-off between the rate and yield of energy production has long been recognized as an evolutionary dilemma, and organisms frequently have cells with different metabolic profiles-some cells with high OXPHOS and others with high glycolysis [3]. It is conceivable that tumors have multiple compartments with different modes of metabolism in order to maximize the amount and rate of energy production. However, the field of cancer metabolism has been focused on determining the predominant metabolic phenotype of cancer cells with little efforts devoted to intra-tumoral metabolic heterogeneity.

In 1924, Otto Warburg described that cancer cells *in vitro* consume far more glucose than normal cells and primarily metabolize it to lactate even in the presence of adequate oxygen, a process termed aerobic glycolysis. He hypothesized that the common feature of all cancer cells was mitochondrial metabolic defects. Mitochondrial abnormalities led to this enhanced dependence on aerobic glycolysis, and this has been named the “Warburg effect” [4]. Subsequent studies have confirmed that certain cancer cells in culture, in the presence of high glucose concentrations, undergo glycolysis even in a high oxygen environment [56]. Further, mutations in components of the TCA cycle, fumarate hydratase, and succinate dehydrogenase, have been described in leiomyomas and pheochromocytomas [78]. However,

the majority of human cancers do not have this reduced mitochondrial metabolism. A study that looked at composite data from 31 cancer cell lines and measured ATP production through OXPHOS and glycolysis found that glycolysis contributed only 17% of the total ATP generation [9]. They concluded that cancer cells are not glycolytic in general; although *in vivo* some tumors may be glycolytic due to their hypoxic environment. Other studies have demonstrated that mitochondrial respiration is not impaired in cancer cells [1011], with some showing that cancer cells depend on the TCA cycle and OXPHOS for the majority of their ATP needs [1213]. In sum, neoplastic tumors have a far more complex metabolic landscape than universal glycolysis.

Neoplastic cells and adjacent non-neoplastic tumor cells may have different, yet interdependent metabolic phenotypes creating a metabolic ecosystem. A multi-compartment model for neoplastic tumor metabolism *in vivo* has been proposed [2141516]. In this metabolic ecosystem, neoplastic cells metabolically re-program neighboring non-neoplastic tumor cells to a glycolytic phenotype; these non-neoplastic cells produce and release monocarboxylates (lactate and ketone bodies) [2]. These metabolites are then taken up by neighboring neoplastic cells for the TCA cycle and OXPHOS, to generate ATP within the neoplastic cells. Thus, this process represents metabolic coupling with transfer of catabolites from non-neoplastic tumor cells to neoplastic cells [14]. It has been demonstrated that multi-compartment metabolism occurs *in vivo* in epithelial malignancies using immunohistochemical metabolic markers like MCT4 for glycolysis and reactive oxygen species (ROS) and MCT1 and TOMM20 for OXPHOS, along with hyperpolarized pyruvate assays in tumor samples [1718]. However, the metabolic ecosystem of lymphoproliferative disorders including diffuse large B-cell lymphomas (DLBCL) is unknown.

DLBCL is the most common histologic subtype of lymphoma in the United States [19]. A number of genetic abnormalities are found in DLBCL including overexpression of BCL2 and BCL6. The *MYC* gene (8q24) is rearranged in 5–15% cases and is associated with very aggressive disease [20]. Particularly aggressive subtypes of DLBCL are the so-called ‘double-hit’ lymphomas. These are defined as those with concurrent rearrangement of *MYC* and *BCL2* or *BCL6* [21]. *MYC* induces the expression of MCT1 which is the main cellular importer of lactate [22]. DLBCL is very aggressive, requiring systemic chemo-immunotherapy at diagnosis [2324] and the 10-year overall survival is estimated at 43.5% with the standard rituximab, cyclophosphamide, doxorubicin, vincristine, prednisone (R-CHOP) regimen [24]. However, DLBCL tumors display great clinical and molecular heterogeneity, with significant variation in outcomes.

The molecular heterogeneity in DLBCL has been investigated with the help of gene expression profiling (GEP), identifying unique gene signatures in subsets of patients. One landmark study identified two biologically distinct subtypes of DLBCL, namely the germinal center type (GC) type (better prognosis) and the activated B-cell (ABC) type, which correlated with more advanced stages of B-cell differentiation [25]. The role of non-neoplastic stromal cells in DLBCL was highlighted in a study, where the tumor microenvironment was found to better predict survival and hence can be used as a prognostic biomarker [26]. This study identified three unique gene expression signatures, namely “germinal-center B cell,” “stromal-1” and “stromal-2”. The latter two signatures reflected

elements in the tumor microenvironment. The “stromal-1” signature (prognostically favorable) included genes encoding for extra-cellular matrix proteins and were infiltrated by myeloid lineage cells including tumor-associated macrophages. The “stromal-2” signature (prognostically unfavorable), was regarded to be an ‘angiogenic switch’ and was associated with increased tumor blood vessel density. Finally, in another study, the consensus cluster classification (CCC) scheme identified three subtypes of DLBCL through molecular profiling: an ‘OXPHOS’ cluster significantly enriched in genes regulating oxidative phosphorylation, mitochondrial membrane potential, and the electron transport chain; a ‘B-cell receptor (BCR)/proliferation cluster,’ rich in genes involved in the BCR signaling axis and cell cycle regulation, including CDK2 and MCM; and third an ‘HR’ (host response) cluster that was characterized by the associated host response rather than the neoplastic cells themselves [27]. A subsequent study revealed that the OXPHOS DLBCL cluster was poorly responsive to conventional agents targeting the BCR signaling axis [28]. Along with enhanced mitochondrial energy transduction, these OXPHOS tumors showed increased nutrient carbon incorporation into the TCA cycle. However, although these studies showed that the tumor microenvironment and the metabolic phenotype of the neoplastic cells are both prognostically important, they did not elucidate the individual metabolic phenotypes of the neoplastic and non-neoplastic tumor cells in situ and the potential metabolic interactions between them. The objective of the study was to determine the metabolic profiles of the different cell types found in DLBCL tumors.

Broadly, the architecture of a lymph node is based on a reticular meshwork comprised of fibroblastic reticular cells (FRCs) which are spindle-shaped, stellate or elongated and their fibers [29], dividing the lymphoid lobule into compartments, which are populated by lymphocytes, macrophages, antigen-presenting cells (APCs, e.g. dendritic cells), plasma cells, and occasional neutrophils [30]. Circulating B-lymphocytes enter the lymph node and home in to the primary follicle. In response to antigens presented by APCs, they then proliferate to form a germinal center with a surrounding mantle of displaced resting B-lymphocytes to form a secondary follicle. Malignant lymph nodes display neoplastic transformation of the lymphocytes, with effacement of the normal lymph node architecture and the presence of adjacent non-neoplastic reactive lymphocytes. The non-neoplastic stromal cells in DLBCL include tumor-associated macrophages, fibroblasts, plasma cells, neutrophils and blood vessels.

The immunohistochemical biomarkers of metabolism that were used in the current study are monocarboxylate transporter 4 (MCT4), monocarboxylate transporter 1 (MCT1), TP53 induced glycolysis and apoptosis regulator (TIGAR) and Translocase of the Outer Mitochondrial Membrane (TOMM20). The monocarboxylate transporters are membrane proteins involved in facilitated transport (proton-linked passive symport) of lactate and other high-energy metabolites such as pyruvate and ketones [3132]. This transport can be bidirectional, driven by concentration gradients, they are differentially expressed in tissues, and are regulated by oxygen and nutrient availability [33]. MCT4, the chief transporter of glycolysis-derived lactate out of the cell, is regarded as a biomarker for reactive oxygen species (ROS), glycolysis and lactate efflux [31]. MCT4 is upregulated by oxidative stress via HIF1A [34]. HIF1A also induces programmed death ligand 1 (PD-L1) expression, which contributes to tumoral immune escape [3536]. Monocarboxylate transporter 1 (MCT1) is

involved in the uptake of lactate into skeletal muscle and other tissues [37] and is specifically upregulated in OXPHOS-rich tissues, particularly under conditions of glucose deprivation [38]. Of particular interest in DLBCL, the transcription of MCT1 is controlled by *MYC* and has been shown to be elevated in neoplasms driven by *MYC* [3922]. Disruption of MCT1 function eventually leads to damage of mitochondrial membrane/apoptosis and generation of oxidative stress via intracellular accumulation of lactate which disrupts numerous metabolic processes [22]. TIGAR is a fructose 2,6 bisphosphatase that reduces glycolytic flux and enhances lactate utilization upregulating MCT1 and increasing OXPHOS [1640]. TOMM20, a member of the outer membrane translocator complex plays a critical role in the recognition, sorting and import of precursor proteins from cytosol to mitochondria [4142]. It's expression correlates with mitochondrial biomass and OXPHOS activity [4344].

The objective of this study was to characterize the metabolic phenotype of the different cells that constitute human DLBCL tumors. We hypothesize that neoplastic lymphocytes in human DLBCL exhibit a mitochondrial or OXPHOS metabolic phenotype, whereas the surrounding non-neoplastic stromal elements express markers of ROS and glycolysis.

METHODS

Tissue samples

Immunohistochemistry was performed using the horseradish immunoperoxidase method to stain 5-micron-thick paraffin-embedded tissue samples as previously described [16]. Briefly, for single labeling immunohistochemistry, antigen retrieval was performed on the Ventana Discovery ULTRA staining platform using Discovery CCI (Ventana cat#950-500) for a total application time of 64 minutes. Primary immunostaining was performed using (insert antibodies here). Secondary immunostaining used a Horseradish Peroxidase (HRP) multimer cocktail (Ventana cat#760-500) and immune complexes were visualized using the ultraView Universal DAB (diaminobenzidine tetrahydrochloride) Detection Kit (Ventana cat#760-500). Slides were then washed with a Tris based reaction buffer (Ventana cat#950-300) and stained with Hematoxylin II (Ventana cat #790-2208) for 8 minutes. Double-labeling on paraffin sections was performed by manual staining after antigen retrieval using an electric pressure cooker. For dual labeling immunohistochemistry, rabbit anti-MCT4 or anti-MCT1 and mouse anti-CD68 were incubated together for one hour at room temperature. After washing in PBS, antibody binding was detected with anti-rabbit-horse radish peroxidase and anti-mouse alkaline phosphatase conjugates (Jackson ImmunoResearch, West Grove, PA). Development was performed first using alkaline phosphatase reagent Vector Red (Vector Labs, Burlingame, CA), followed by peroxidase reagent 3,3' diaminobenzidine (Dako).

Dual labeling immunofluorescence was done in a similar manner except secondary reagents were goat anti-rabbit Alexa Fluor 488 and goat anti-mouse Alexa Fluor 568. Nuclei were counterstained with Dapi and coverslipped with ProLong Gold anti-fade (Invitrogen, Thermo Fisher, Carlsbad, CA). Images were captured using a Zeiss Meta-510 or Nikon A1R confocal microscope.

The following antibodies were used: TOMM20 (F-10; sc-17764; Santa Cruz Biotechnology, Santa Cruz, CA), MCT4 (three antibodies were used: 1) rabbit antibody; 19-mer peptide sequence CKAEPEKNGEVVHTPETSV-cooh; YenZym Antibodies, South San Francisco, CA, 2) rabbit antibody sc-50329 used for double labeling with CD68 and MCT4 (D-1) mouse antibody sc-376140 used for double labeling with PD-L1; Santa Cruz Biotechnology,Santa Cruz, CA.), MCT1 (rabbit antibody; 19-mer peptide sequence CSPDQKDTEGGPKEEESPV-cooh; YenZym Antibodies, South San Francisco, CA), CD68 (M0814; Dako Corp., Carpinteria, CA), PD-L1 (E1L3N; Cell Signaling Technology; Danvers, MA) and TIGAR (ab62533, Abcam, Cambridge, MA).

This study was conducted with institutional review board approval. We identified consecutive patients diagnosed with DLBCL at our institution from 2009–15 with available diagnostic tissue samples. All patients were treated at Thomas Jefferson University Hospital as the single institution. All samples are from the initial diagnosis of diffuse large B cell lymphoma. One patient had transformed diffuse large B cell lymphoma and the sample studied was the initial diagnosis of transformed disease. These patients comprised Cohort 1 (n = 28). Only 26 patients had evaluable MCT1 staining. In addition, samples were double-stained for CD68, a marker for macrophages, along with MCT1 or MCT4.

The subjects in Cohort 1 (n=28) were not routinely tested for double-hit lymphoma markers upfront. In order to study the staining pattern in diffuse large B-cell lymphoma of the double-hit subtype, we subsequently identified 5 additional patients (diagnosed after 2015) with the double-hit subtype of DLBCL. These patients comprised Cohort 2. Staining patterns were investigated in this second cohort of five patients and were analyzed separately.

In DLBCL samples in this study, the neoplastic lymphocytes are denoted as cancer cells (C). The adjacent tumor microenvironment includes non-neoplastic reactive lymphocytes, which are denoted as RL. Tumor-associated macrophages (TAM) as well as other cancer-associated stroma (CAS), which can include fibroblasts, antigen presenting cells (APCs), plasma cells, and neutrophils constitute the tumor microenvironment.

Immunostains were graded by two pathologists (blinded to the clinical characteristics of the study subject) on a scale of 0, 1+, or 2+ for each cell type, based on the intensity and percentage of immunoreactivity as follows: 0 for no detectable staining in >/= 50% of cells; 1+ for faint to moderate staining in >/= 50% of cells, and 2+ for strong staining in >50% of cells. Two pathologists confirmed the diagnosis of diffuse large B cell lymphoma on all samples.

Finally, tissue from biopsies of non-neoplastic lymph nodes from 18 randomly selected control patients were similarly stained with MCT4, TOMM20, and MCT1. These samples were evaluated and graded by similar pathologic criteria as the neoplastic samples. In these non-neoplastic samples, lymphocytes were denoted as (L), while in the surrounding stroma, macrophages were denoted as (M), and non-macrophage stroma (FRCs, APCs, plasma cells, neutrophils) collectively denoted as NMS.

Patient data—Available clinical data collected by chart review included age, sex, stage, SUVmax (SUVm) on PET/CT scan, treatment regimen, response to rituximab/anthracycline containing first-line therapy (first complete remission or CR1, first partial remission or PR, refractory), relapse, extra-nodal involvement, and evidence of transformation from a different underlying lymphoma (follicular lymphoma or Hodgkin disease) as well as the revised International Prognostic Index (R-IPI). Zero risk factors in the R-IPI constitutes a "very good" prognostic group, 1 or 2 risk factors constitute a "good" prognostic group and 3, 4, or 5 risk factors constitute a "poor" risk group as previously described[45].

Pathologic and laboratory data collected by chart review included LDH at diagnosis, Ki-67 index, GC (germinal center) versus ABC (activated B-cell) subtype of DLBCL by immunohistochemistry and presence of *MYC* gene rearrangement (when performed). Ki-67 >70% was regarded as the cut-off for a higher proliferative index.

Statistics—Fisher's exact test and the chi;^{2} test were used to test for association among categorical variables.

RESULTS

Baseline patient characteristics: Among the 28 DLBCL patients studied in Cohort 1, (Table 1), 43% were male. The median age for the cohort was 60.5 years. Of the patients who had available LDH values at diagnosis (n=20), 8/20 or 40% had elevated values. Extra-nodal sites were involved in 22/28 or 79% of patients, and 7/28 or 25% had undergone transformation from follicular lymphoma or Hodgkin lymphoma. Among patients who underwent PET/CT scans prior to frontline therapy (n=20), the median SUV max was 19.4 (range 3.5 – 42.2). Ki-67 was elevated (greater than 70%) in 8 of 17 samples (47%) with available values. In 25 of 28 patients data were available to allow characterization as GC or ABC by immunohistochemistry, with 8 GC and 17 non-GC patients. The majority (82%) of patients were Stage IV at diagnosis. *MYC* status was available for only five patients in this cohort, and only one was positive for *MYC* rearrangement by cytogenetics/FISH.

In the second cohort of exclusively double-hit diffuse large B-cell lymphoma patients or Cohort 2 (n=5), all patients were *MYC* positive and had either a *BCL2* or a *BCL6* rearrangement by cytogenetics/FISH. The baseline characteristics of patients in this cohort are summarized in Table 2.

Metabolic signatures of DLBCL tumor samples

Cohort 1

Neoplastic lymphocytes: In 27 of 28 DLBCL cases (96%), neoplastic lymphocytes (C) stained 2+ for TOMM20, with a single sample staining 1+. MCT4 expression was completely absent in neoplastic lymphocytes (C) in all samples. MCT1 expression in neoplastic lymphocytes (C) was 2+ in 24 samples (92%) of the 26 samples with evaluable staining while the remaining two samples (8%) expressed it at 1+. The staining patterns of neoplastic cells for patients in Cohort 1 are shown in Figures 1–3 and in Tables 3 and 4.

Non-neoplastic resident tumor cells: TOMM20 was either not expressed (46%) or had 1+ expression in 15 samples (54%) in CAS and TAM of DLBCL samples. TOMM20 expression patterns in CAS and TAM were identical. MCT4 expression was 2+ in 13 samples (46%) of CAS and 21 samples (75%) of TAM, and 1+ in the CAS and TAM of the remaining samples. MCT1 was 1+ expressed in 18 samples (69%) of CAS and 19 samples (73%) of TAM. Figure 1A demonstrates MCT4 staining of CAS and TAM from two patient samples. It is apparent that the first sample has a much greater proportion of stromal elements compared to the second sample, however the patterns are identical. Increased levels of MCT4 expression in CAS paralleled increased levels of MCT4 expression in TAM and the staining patterns were concordant ($p<0.07$). Finally, Reactive lymphocytes (RL) in the tumor tissue samples had no MCT4 expression and uniform 1+ TOMM20 expression. MCT1 expression in reactive lymphocytes was 1+ in 22 of 26 samples. The staining patterns for non-neoplastic cells for patients in Cohort 1 are shown in Table 3 and 4.

In summary, neoplastic lymphocytes stained strongly positive for TOMM20 and MCT1, whereas CAS and TAM stained for MCT4 with a distinctively different metabolic phenotype. The composite metabolic profile of neoplastic and non-neoplastic tumor cells in DLBCL samples is shown in Fig 2.

Double-staining of DLBCL samples: DLBCL was stained with both CD68 (green) and MCT4 (red) represented in Fig 1, and demonstrated strong MCT4 uptake on CD68 positive cells (histiocyte or macrophage marker). This highlights that tumor-associated macrophages are MCT4 avid in DLBCL samples.

CD68 (green) and MCT1 (red) double labeling was also performed and a representative example is shown in the right panel of Fig 1B. MCT1 is not expressed by CD68 positive macrophages (TAMs), but is expressed in adjacent neoplastic lymphocytes.

In sum, TAMs are MCT4 avid in DLBCL, while as the neoplastic lymphocytes do not express MCT4.

Cohort 2 (Double-hit subtype)—In the five patients with diffuse large B-cell lymphoma of the double-hit subtype, all had de-novo disease without any cases of transformed disease. There was diffuse and homogenous 2+ staining for MCT1 in cancer cells (C). Stroma and macrophages (CAS and TAM) stained 2+ for MCT4. Interestingly, the stroma was negative for MCT1 in contrast to the mild background MCT1 staining seen in the CAS and TAM of non-double-hit DLBCL.

Double-staining of double-hit DLBCL: Double-staining of one of the five samples was performed with MCT4 (brown) and CD68 (pink) to delineate the identity of the MCT4 positive cells (Fig 3A). The top right panel demonstrates MCT4 uptake in the stroma sparing the neoplastic lymphocytes. The bottom two panels show that the CD68 positive macrophages are MCT4 avid.

Further double-staining was performed with MCT1 (brown) and CD68 (pink) (Fig 3B). Once again the top right panel illustrates avid uptake of MCT1 on the neoplastic

lymphocytes, sparing the stroma. The bottom two panels confirm that CD68 positive macrophages are not MCT1 avid.

Metabolic signatures of non-neoplastic lymph nodes (external controls)

Nine of 18 controls were non-neoplastic lymph nodes obtained from patients with active solid malignancies, while the remainder included non-neoplastic lymph nodes from patients with ulcerative colitis, benign intestinal obstruction, and benign lymph nodes with follicular hyperplasia. Staining patterns were recorded in the following three compartments: non-neoplastic lymphocytes (L), analogous to cancer cells (C) in DLBCL, macrophages (M), analogous to TAM in DLBCL cases and non-macrophage stroma (fibroblastic reticular cells-FRCs, antigen presenting cells-APCs, plasma cells and neutrophils) collectively called NMS, analogous to CAS in DLBCL cases. The staining patterns are described below and summarized in Table 4.

Non-neoplastic Lymphocytes (L): In all control samples (n=18), lymphocytes did not stain for MCT4 at all, either within germinal centers or in inter-follicular regions. This was identical to the DLBCL cases where none of the neoplastic lymphocytes stained for MCT4.

The staining pattern for TOMM20 differed significantly in the non-neoplastic controls versus DLBCL cases. Non-neoplastic lymphocytes (L) had 2+ staining for TOMM20 in only 16.7% of control samples whereas 2+ TOMM20 staining was seen in the neoplastic lymphocytes of 96.4% of the DLBCL cases. Hence, 2+ TOMM20 staining in neoplastic lymphocytes (C) was significantly stronger than in non-neoplastic lymphocytes (L) ($p<0.001$). The majority of (L) stained only 1+ for TOMM20 (72%), and staining was predominantly confined to the active germinal centers. The remaining 11.1% did not take up TOMM20 at all. Fig 4C and Fig 5A, compare the TOMM20 staining patterns in DLBCL cases versus non-neoplastic lymph nodes (controls).

Finally, the MCT1 staining patterns were also significantly different in DLBCL cases and non-neoplastic lymph nodes. (L) in only 11.1% of non-neoplastic lymph nodes stained 2+ for MCT1, compared with 2+ MCT1 staining in neoplastic lymphocytes (C) in 92% of DLBCL cases ($p<0.001$). The majority of L in non-neoplastic lymph nodes stained 1+ for MCT1. Fig 4B and Fig 5, Panel B compare the MCT1 staining patterns in DLBCL cases versus non-neoplastic lymph nodes (controls).

Macrophage (M) and Non-Macrophage stroma (NMS): The pattern of MCT4 staining was significantly different in M and NMS of non-neoplastic lymph nodes compared to the stroma (CAS and TAM) of DLBCL cases. M stained 2+ for MCT4 in only 11% (2 samples) compared to 2+ MCT4 staining in the TAM of 75% of DLBCL cases ($p<0.001$). Furthermore the two MCT4 avid control samples were rich in granulomas, which could explain their metabolic phenotype. Indeed, in 61% of control samples, (M) did not take up MCT4 at all with the remaining 27% staining 1+ for MCT4. This pattern was replicated in NMS of non-neoplastic lymph nodes as well. MCT4 staining patterns are shown side-by-side in DLBCL cases and non-neoplastic control lymph nodes in Figures 4 and 6.

Stromal TOMM20 staining patterns were also different in DLBCL cases versus non-neoplastic lymph nodes. The macrophages (M) in only 1 of 18 samples (6%) of non-neoplastic controls stained 0 for MCT4, whereas in DLBCL casdses, 13 of 28 samples (46%) of TAM stained 0 for TOMM20 ($p<0.01$). Macrophages in non-neoplastic samples (M) stained 0 or 1+ for MCT4 in the majority of cases since it was positive in 8 of 9 samples (89%). Once again the staining pattern in NMS was identical to that in M.

Finally, there were differences in MCT1 staining patterns in DLBCL cases versus non-neoplastic control lymph nodes. In both M and NMS, MCT1 staining was 1+ in 44% and was absent in the remainder except in one sample (6%). In contrast, MCT1 was expressed at 1+ in 73% of CAS and 77% of TAM in DLBCL cases. Staining patterns in DLBCL cases versus controls are compared in Fig 4,5 and 6. DLBCL had co-localization of PD-L1 and MCT4 and increased TIGAR expression in Fig 7 and 8.

In summary, non-neoplastic lymphocytes in control lymph nodes did not express MCT4 and they expressed less TOMM20 and MCT1 than neoplastic lymphocytes in DLBCL cases. On the other hand, the macrophage and non-macrophage stroma in control lymph nodes expressed less MCT4 than TAM and CAS of DLBCL cases. MCT4 is a marker of tumor stromal elements in DLBCL, since it is expressed in DLBCL and is absent in the majority of non-neoplastic lymph nodes.

Ratio of tumor cells to stromal cells

In Cohort 1, the pathologists quantitated the ratio of cancer cells to stromal cells from the H&E tissue sections; 25 patients had evaluable data. The median tumor: stroma ratio (T:S) was 1.00. 12/25 (48%) had T:S>1, 9/25 (36%) had T:S<1 and the remaining 4/25 (16%) had T:S of 1.00. Of note, there was no significant correlation between T:S ratio and achieving a complete remission (CR). Fig 9 demonstrates the tumor: stroma ratio in evaluable samples.

DISCUSSION

We have shown that the neoplastic lymphocytes in the DLBCL samples stained uniformly and strongly with an immunohistochemical marker for oxidative phosphorylation (TOMM20). In contrast, none of the neoplastic lymphocytes in the DLBCL samples stained positively for MCT4, a marker for glycolysis, lactate/ketone transport, and oxidative stress. These staining patterns suggest that, neoplastic lymphocytes in DLBCL undergo a significant degree of mitochondrial oxidative metabolism rather than aerobic glycolysis and thus are able to produce larger amounts of ATP than could be obtained by glycolysis. Conversely, in the tumor stroma (tumor-associated macrophages and cancer-associated stroma), there was either absent or weak TOMM20 expression, whereas MCT4 was strongly expressed. This implies that the tumor stroma as a whole is strongly glycolytic with less mitochondrial respiration (OXPHOS). Furthermore it is likely that the stromal elements are subject to oxidative stress, as indicated by MCT4 positivity [34]. Although the stroma utilizes a less energy efficient pathway for ATP generation, namely aerobic glycolysis; it may have an additional critical role, i.e. production of an important metabolic intermediate (lactate) that can be used by the neighboring neoplastic lymphocytes as an alternative substrate to glucose.

In order to understand the interactions between the glycolytic and OXPHOS compartments in DLBCL, we then investigated markers of the transport of lactate in and out of these compartments, by studying the patterns of MCT1 (lactate importer) and MCT4 (lactate exporter) expression. MCT1 is a marker expressed in tissues undergoing OXPHOS and associated with lactate import or uptake into tissues, whereas, as mentioned previously, MCT4 is a marker of lactate export and glycolysis. MCT1 staining was significantly greater in the neoplastic lymphocytes compared to the tumor stroma (CAS and TAM), whereas MCT4 staining was significantly greater in TAM/CAS compared to neoplastic lymphocytes. This suggests that metabolic heterogeneity exists between OXPHOS and glycolytic compartments, with lactate acting as the metabolite that is produced in the stroma, and taken up by the neoplastic lymphocytes through monocarboxylate transporters, and eventually metabolized to ATP through OXPHOS. In this way, the tumor is able to generate alternative substrates to glucose that can be metabolized for ATP production, a phenomenon that could be important in conditions of glucose deprivation. Furthermore, it is possible that the products of stromal glycolytic metabolism are taken up by neighboring neoplastic lymphocytes and utilized as metabolic substrates and building blocks for cellular biomass. Hence, there is metabolic heterogeneity between multiple cellular compartments within a tumor, which may help it to adapt to its metabolic needs.

Thus, we have shown that the metabolic landscape of neoplastic cells and their surrounding stromal elements is more complex than the homogeneous aerobic glycolysis suggested by the Warburg effect. It is critical for tumors to maintain or increase cellular biomass by generating a sufficient amount of ATP efficiently and recycling metabolites. Metabolic compartmentalization within a tumor might allow ATP production and biomass building blocks. We demonstrate for the first time that two closely interlinked metabolic compartments exist in human DLBCL, namely the OXPHOS and glycolytic compartments. Furthermore, we suggest, based on the staining pattern of monocarboxylate transporters, that metabolites produced by glycolysis in tumor stroma (lactate) are taken up and utilized by neoplastic lymphocytes to generate ATP through oxidative phosphorylation. This newly proposed paradigm of tumor-stromal metabolic heterogeneity in DLBCL is illustrated in Fig 10A and 10B. Conversely, non-neoplastic lymphatic tissue, which has very different metabolic requirements from neoplastic lymph nodes has a different staining pattern.

To confirm that the observed staining patterns in DLBCL samples were characteristic for neoplastic tissue, we investigated the metabolic staining patterns in 18 non-neoplastic control lymph nodes. Substantial differences were observed in the staining patterns of TOMM20, MCT4 and MCT1 between neoplastic and non-neoplastic tissue. Overall, non-neoplastic lymphocytes were significantly less positive for TOMM20 and MCT1 than cancer cells. Hence, the non-neoplastic lymphocytes showed no evidence of the OXPHOS phenotype that was observed in neoplastic lymphocytes. Similarly, MCT4 staining was significantly less prominent in both macrophages and non-macrophage stroma in the control lymph nodes, compared to the TAM and CAS of the DLBCL cases. Hence, in tumors MCT4 was strongly positive only in the stroma surrounding neoplastic lymphocytes, and this marker of oxidative stress, glycolysis, and lactate export can be regarded as a marker for tumor-associated stroma. It is possible that there is a specific effect of neoplastic lymphocytes in transforming the metabolic pathways of normal stromal elements into a

glycolytic phenotype, with the production of energy-rich substrates such as lactate as an end-product. Lactate may not be an important metabolite in non-neoplastic lymph nodes compared to neoplastic lymph nodes since there is a paucity of lactate exporters in the normal stroma and lactate importers in the non-neoplastic lymphocytes in control samples. Fig 10B summarizes the differences in metabolic compartmentalization in neoplastic and non-neoplastic lymph nodes.

MCT1 transcription is regulated by *MYC*. We investigated MCT1 expression along with TOMM20 and MCT4 in a second cohort (Cohort 2) of five patients with double-hit lymphoma subtype of DLBCL who were all positive for the *MYC* rearrangement. Interestingly in all samples, the staining pattern of MCT1, MCT4 and TOMM20 was similar in double hit lymphomas to that in non-*MYC* positive DLBCL. Hence, varied DLBCL genotypes lead to similar metabolic phenotypes. This is consistent with the fact that many oncogenes can alter cellular metabolism in a similar way [46]. However, the precise role of *MYC, BCL2, BCL6* and other genetic pathways in multi-compartment metabolism will have to be defined experimentally.

Finally, we observed large variation in the proportion of neoplastic lymphocytes and stromal elements in different DLBCL samples. A greater number of cancer cells compared to stroma was only found in half of the cases of DLBCL which highlights that TAM/CAS are substantial components in DLBCL tumors. Given that neoplastic lymphocytes undergo OXPHOS metabolism and TAM/CAS undergo aerobic glycolysis, it is conceivable that the relative proportions of neoplastic lymphocytes and stromal elements could influence the overall metabolic behavior of the tumor. However, we were not able to establish any prognostic or predictive value for the T:S ratio in this small cohort of patients.

The limitations of this study include small sample size and the retrospective nature of the analysis. It is unclear why several subjects had low SUV in their PET scans although they are within the range of SUV described in the literature [4748]. The poor outcomes in this cohort may reflect this institution's case mix with referrals of patients who had relapsed disease or were refractory to treatment. Another limitation is that our analysis is based on fixed tissue samples, which provide a window into tumor metabolism *in vivo* but do not allow the observation of sequential events in the process of metabolic reprogramming. Future studies are needed to elucidate the mechanisms that induce multi-compartment metabolism in lymphomas.

Our findings of tumor-stromal metabolic coupling in DLBCL support testing new therapeutic targets. In recent years there has been renewed interest in uncovering genes, which act as metabolic switches in tumors. The monocarboxylate transporters are located on the membrane of cells and thus are ideal drug targets for metabolic inhibition. Particularly in *MYC*-driven tumors like double-hit lymphomas, MCT1 blockade may be a therapeutic target. Finally, metformin blocks Complex I of the mitochondrial respiratory transport chain and its use in diabetic patients is associated with an increased response to anti-lymphoma therapy in DLBCL[49]. Disruption of neoplasticstromal metabolic coupling at various levels could retard tumor metabolism, growth and survival.

In summary, we have demonstrated that multi-compartment metabolism exists in DLBCL, a disorder in which the prognostic importance of stromal and metabolic signatures has already been demonstrated through gene expression profiling. We hypothesize that neoplastic cells metabolically reprogram the surrounding stroma to undergo aerobic glycolysis. Lactate which is the end-product of glycolysis is generated in the stroma and taken up by neighboring neoplastic cells, which utilize these substrates to generate ATP through the TCA cycle. A highly proliferative aggressive tumor is thus metabolically adapted to survive in nutrient- and oxygen-poor conditions. Further elucidation of the genes involved in metabolic reprogramming and regulation of nutrient transporters may unmask important therapeutic targets in DLBCL, particularly for tumors poorly responsive to current chemo-immunotherapy regimens. *MYC*-driven tumors with strong MCT1 positivity could be effective targets for MCT1 blocking agents. Metabolic heterogeneity of neoplastic and non-neoplastic tumor cells by targeting membrane receptors or more proximal pathways could disrupt nutrient and energy resources for these tumors and retard their growth significantly. Further investigation in these areas should be actively pursued.

Acknowledgments

The National Cancer Institute of the National Institutes of Health under Award Numbers K08 CA175193 and P30CA056036 supported this work. Funding was used to provide material support for laboratory testing.

BIBLIOGRAPHY

1. DeBerardinis RJ, Chandel NS. Fundamentals of cancer metabolism. Sci Adv. 2016; 2:e1600200. [PubMed: 27386546]
2. Martinez-Outschoorn UE, Peiris-Pages M, Pestell RG, Sotgia F, Lisanti MP. Cancer metabolism: a therapeutic perspective. Nat Rev Clin Oncol. 2017; 14:11–31. [PubMed: 27141887]
3. Pfeiffer T, Schuster S, Bonhoeffer S. Cooperation and competition in the evolution of ATP-producing pathways. Science. 2001; 292:504–7. [PubMed: 11283355]
4. Warburg O. On the origin of cancer cells. Science. 1956; 123:309–14. [PubMed: 13298683]
5. Medina MA, Sanchez-Jimenez F, Marquez FJ, Perez-Rodriguez J, Quesada AR, Nunez de Castro I. Glutamine and glucose as energy substrates for Ehrlich ascites tumour cells. Biochem Int. 1988; 16:339–47. [PubMed: 3365266]
6. Schmidt H, Siems W, Muller M, Dumdey R, Rapoport SM. ATP-producing and consuming processes of Ehrlich mouse ascites tumor cells in proliferating and resting phases. Exp Cell Res. 1991; 194:122–7. [PubMed: 1707821]
7. Astuti D, Latif F, Dallol A, et al. Gene mutations in the succinate dehydrogenase subunit SDHB cause susceptibility to familial pheochromocytoma and to familial paraganglioma. Am J Hum Genet. 2001; 69:49–54. [PubMed: 11404820]
8. King A, Selak MA, Gottlieb E. Succinate dehydrogenase and fumarate hydratase: linking mitochondrial dysfunction and cancer. Oncogene. 2006; 25:4675–82. [PubMed: 16892081]
9. Zu XL, Guppy M. Cancer metabolism: facts, fantasy, and fiction. Biochem Biophys Res Commun. 2004; 313:459–65. [PubMed: 14697210]
10. Fantin VR, St-Pierre J, Leder P. Attenuation of LDH-A expression uncovers a link between glycolysis, mitochondrial physiology, and tumor maintenance. Cancer Cell. 2006; 9:425–34. [PubMed: 16766262]
11. Moreno-Sanchez R, Rodriguez-Enriquez S, Marin-Hernandez A, Saavedra E. Energy metabolism in tumor cells. FEBS J. 2007; 274:1393–418. [PubMed: 17302740]
12. Guppy M, Leedman P, Zu X, Russell V. Contribution by different fuels and metabolic pathways to the total ATP turnover of proliferating MCF-7 breast cancer cells. Biochem J. 2002; 364:309–15. [PubMed: 11988105]

13. Kallinowski F, Vaupel P, Runkel S, et al. Glucose uptake, lactate release, ketone body turnover, metabolic micromilieu, and pH distributions in human breast cancer xenografts in nude rats. Cancer Res. 1988; 48:7264–72. [PubMed: 3191497]
14. Pavlides S, Whitaker-Menezes D, Castello-Cros R, et al. The reverse Warburg effect: aerobic glycolysis in cancer associated fibroblasts and the tumor stroma. Cell Cycle. 2009; 8:3984–4001. [PubMed: 19923890]
15. Martinez-Outschoorn UE, Lin Z, Trimmer C, et al. Cancer cells metabolically "fertilize" the tumor microenvironment with hydrogen peroxide, driving the Warburg effect: implications for PET imaging of human tumors. Cell Cycle. 2011; 10:2504–20. [PubMed: 21778829]
16. Ko YH, Domingo-Vidal M, Roche M, et al. TIGAR Metabolically Reprograms Carcinoma and Stromal Cells in Breast Cancer. J Biol Chem. 2016
17. Curry JM, Tuluc M, Whitaker-Menezes D, et al. Cancer metabolism, stemness and tumor recurrence: MCT1 and MCT4 are functional biomarkers of metabolic symbiosis in head and neck cancer. Cell Cycle. 2013; 12:1371–84. [PubMed: 23574725]
18. Johnson JM, Lai SY, Cotzia P, et al. Mitochondrial Metabolism as a Treatment Target in Anaplastic Thyroid Cancer. Semin Oncol. 2015; 42:915–22. [PubMed: 26615136]
19. Morton LM, Wang SS, Devesa SS, Hartge P, Weisenburger DD, Linet MS. Lymphoma incidence patterns by WHO subtype in the United States, 1992–2001. Blood. 2006; 107:265–76. [PubMed: 16150940]
20. Zhou K, Xu D, Cao Y, Wang J, Yang Y, Huang M. C-MYC aberrations as prognostic factors in diffuse large B-cell lymphoma: a meta-analysis of epidemiological studies. PLoS One. 2014; 9:e95020. [PubMed: 24740248]
21. Jaffe ES, Pittaluga S. Aggressive B-cell lymphomas: a review of new and old entities in the WHO classification. Hematology Am Soc Hematol Educ Program. 2011; 2011:506–14. [PubMed: 22160082]
22. Doherty JR, Yang C, Scott KE, et al. Blocking lactate export by inhibiting the Myc target MCT1 Disables glycolysis and glutathione synthesis. Cancer Res. 2014; 74:908–20. [PubMed: 24285728]
23. Armitage JO. My treatment approach to patients with diffuse large B-cell lymphoma. Mayo Clin Proc. 2012; 87:161–71. [PubMed: 22305028]
24. Coiffier B, Thieblemont C, Van Den Neste E, et al. Long-term outcome of patients in the LNH-98. 5 trial, the first randomized study comparing rituximab-CHOP to standard CHOP chemotherapy in DLBCL patients: a study by the Groupe d'Etudes des Lymphomes de l'Adulte. Blood. 2010; 116:2040–5. [PubMed: 20548096]
25. Alizadeh AA, Eisen MB, Davis RE, et al. Distinct types of diffuse large B-cell lymphoma identified by gene expression profiling. Nature. 2000; 403:503–11. [PubMed: 10676951]
26. Lenz G, Wright G, Dave SS, et al. Stromal gene signatures in large-B-cell lymphomas. N Engl J Med. 2008; 359:2313–23. [PubMed: 19038878]
27. Monti S, Savage KJ, Kutok JL, et al. Molecular profiling of diffuse large B-cell lymphoma identifies robust subtypes including one characterized by host inflammatory response. Blood. 2005; 105:1851–61. [PubMed: 15550490]
28. Caro P, Kishan AU, Norberg E, et al. Metabolic signatures uncover distinct targets in molecular subsets of diffuse large B cell lymphoma. Cancer Cell. 2012; 22:547–60. [PubMed: 23079663]
29. Gretz JE, Kaldjian EP, Anderson AO, Shaw S. Sophisticated strategies for information encounter in the lymph node: the reticular network as a conduit of soluble information and a highway for cell traffic. J Immunol. 1996; 157:495–9. [PubMed: 8752893]
30. Willard-Mack CL. Normal structure, function, and histology of lymph nodes. Toxicol Pathol. 2006; 34:409–24. [PubMed: 17067937]
31. Brooks GA. Cell-cell and intracellular lactate shuttles. J Physiol. 2009; 587:5591–600. [PubMed: 19805739]
32. Martinez-Outschoorn UE, Whitaker-Menezes D, Valsecchi M, et al. Reverse Warburg effect in a patient with aggressive B-cell lymphoma: is lactic acidosis a paraneoplastic syndrome? Semin Oncol. 2013; 40:403–18. [PubMed: 23972703]
33. Bergersen LH, Eid T. Monocarboxylate transport matters. N Engl J Med. 2014; 371:1931–2. [PubMed: 25390745]

34. Ullah MS, Davies AJ, Halestrap AP. The plasma membrane lactate transporter MCT4, but not MCT1, is up-regulated by hypoxia through a HIF-1alpha-dependent mechanism. J Biol Chem. 2006; 281:9030–7. [PubMed: 16452478]
35. Noman MZ, Desantis G, Janji B, et al. PD-L1 is a novel direct target of HIF-1alpha, and its blockade under hypoxia enhanced MDSC-mediated T cell activation. J Exp Med. 2014; 211:781–90. [PubMed: 24778419]
36. Barsoum IB, Smallwood CA, Siemens DR, Graham CH. A mechanism of hypoxia-mediated escape from adaptive immunity in cancer cells. Cancer Res. 2014; 74:665–74. [PubMed: 24336068]
37. McCullagh KJ, Poole RC, Halestrap AP, O'Brien M, Bonen A. Role of the lactate transporter (MCT1) in skeletal muscles. Am J Physiol. 1996; 271:E143–50. [PubMed: 8760092]
38. De Saedeleer CJ, Porporato PE, Copetti T, et al. Glucose deprivation increases monocarboxylate transporter 1 (MCT1) expression and MCT1-dependent tumor cell migration. Oncogene. 2014; 33:4060–8. [PubMed: 24166504]
39. Doherty JR, Cleveland JL. Targeting lactate metabolism for cancer therapeutics. J Clin Invest. 2013; 123:3685–92. [PubMed: 23999443]
40. Bensaad K, Tsuruta A, Selak MA, et al. TIGAR, a p53-inducible regulator of glycolysis and apoptosis. Cell. 2006; 126:107–20. [PubMed: 16839880]
41. Wurm CA, Neumann D, Lauterbach MA, et al. Nanoscale distribution of mitochondrial import receptor Tom20 is adjusted to cellular conditions and exhibits an inner-cellular gradient. Proc Natl Acad Sci U S A. 2011; 108:13546–51. [PubMed: 21799113]
42. Yamamoto H, Itoh N, Kawano S, et al. Dual role of the receptor Tom20 in specificity and efficiency of protein import into mitochondria. Proc Natl Acad Sci U S A. 2011; 108:91–6. [PubMed: 21173275]
43. Yano M, Kanazawa M, Terada K, Takeya M, Hoogenraad N, Mori M. Functional analysis of human mitochondrial receptor Tom20 for protein import into mitochondria. J Biol Chem. 1998; 273:26844–51. [PubMed: 9756929]
44. Yano M, Terada K, Mori M. Mitochondrial import receptors Tom20 and Tom22 have chaperone-like activity. J Biol Chem. 2004; 279:10808–13. [PubMed: 14699115]
45. Sehn LH, Berry B, Chhanabhai M, et al. The revised International Prognostic Index (R-IPI) is a better predictor of outcome than the standard IPI for patients with diffuse large B-cell lymphoma treated with R-CHOP. Blood. 2007; 109:1857–61. [PubMed: 17105812]
46. Levine AJ, Puzio-Kuter AM. The control of the metabolic switch in cancers by oncogenes and tumor suppressor genes. Science. 2010; 330:1340–4. [PubMed: 21127244]
47. Gallicchio R, Mansueto G, Simeon V, et al. F-18 FDG PET/CT quantization parameters as predictors of outcome in patients with diffuse large B-cell lymphoma. Eur J Haematol. 2014; 92:382–9. [PubMed: 24428392]
48. Minamimoto R, Fayad L, Advani R, et al. Diffuse Large B-Cell Lymphoma: Prospective Multicenter Comparison of Early Interim FLT PET/CT versus FDG PET/CT with IHP, EORTC, Deauville, and PERCIST Criteria for Early Therapeutic Monitoring. Radiology. 2016; 280:220–9. [PubMed: 26854705]
49. Alkhatib Y, Abdel Rahman Z, Kuriakose P. Clinical impact of metformin in diabetic diffuse large B-cell lymphoma patients: a case-control study. Leuk Lymphoma. 2016:1–5.

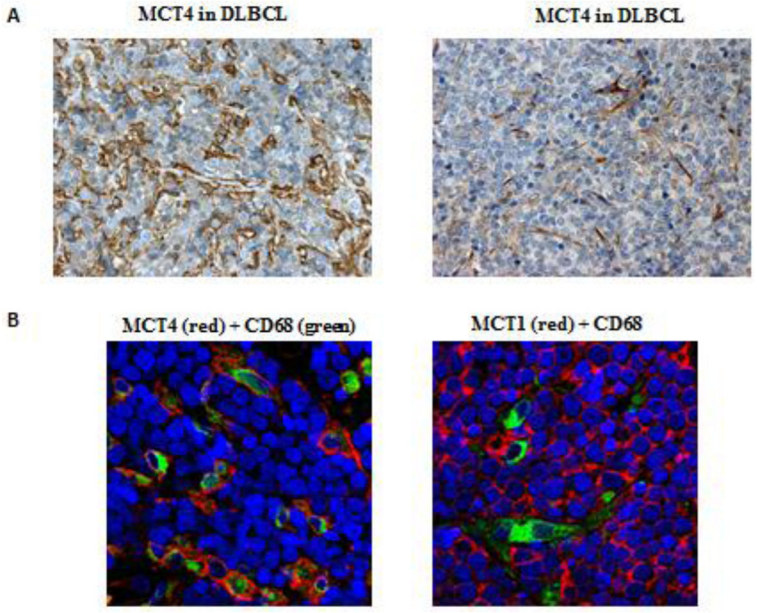

Fig 1. MCT4, MCT1 and CD68 staining in DLBCL

Expression of MCT4 in the tumor-associated macrophages (TAM) and cancer-associated stroma (CAS) in two patient samples of diffuse large B-cell lymphoma. Note that the neoplastic cells in DLBCL do not stain for MCT4 while, stromal components are strongly positive (A). CD68 positive tumor-associated macrophages (TAM) are positive for MCT4 while, as they are negative for MCT1 in DLBCL samples (B).

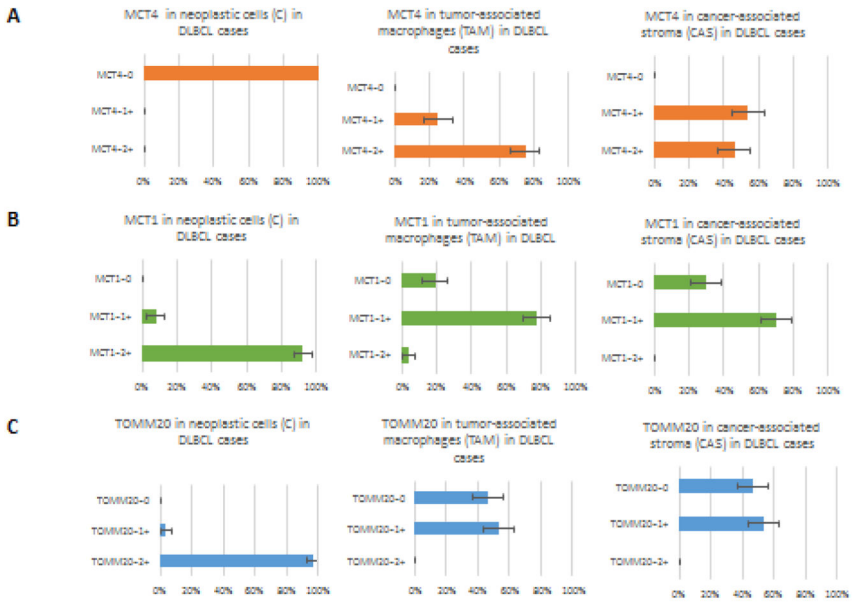

Fig 2. MCT4, MCT1 and TOMM20 staining in neoplastic cells, tumor associated macrophages and cancer-associated stroma in DLBCL

Composite metabolic profile of neoplastic lymphocytes and surrounding stromal elements (tumor-associated macrophages and cancer-associated stroma) in diffuse large B-cell lymphoma. Note that cancer cells express MCT1 and TOMM20 highly and have low MCT4 expression. Conversely, Macrophages and other stroma (TAMs and CAS) have low MCT1 and TOMM20 while, as MCT4 expression is high.

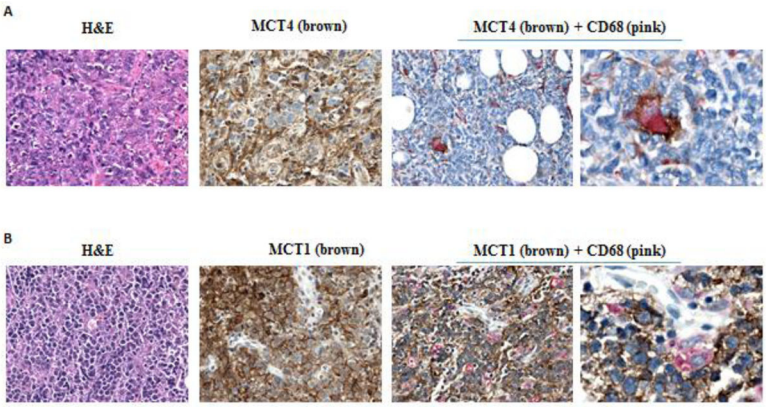

Fig 3. MCT4, MCT1 and CD68 staining in double-hit DLBCL

H&E, MCT4 staining and double-staining with MCT4 (brown) and CD68 (pink) are shown (A). Note that cancer cells are negative for MCT4 while as the stroma is positive and on double labeling that the CD68 positive macrophages are also MCT4 positive. H&E, MCT1 staining and double staining of MCT1 (brown) and CD68 (pink) in double hit DLBCL (B). Note that the neoplastic lymphocytes are MCT1 positive whereas CD68 positive macrophages are negative for MCT1.

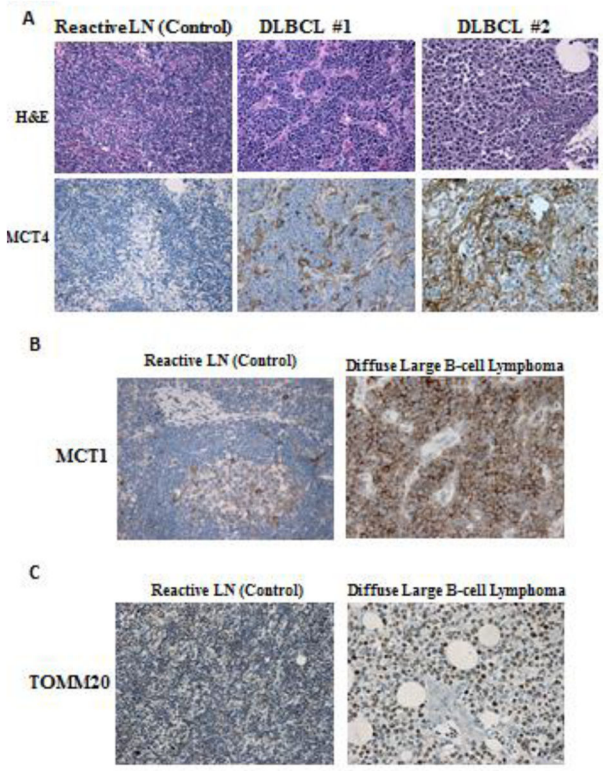

Fig 4. MCT4, MCT1 and TOMM20 staining in reactive non-neoplastic lymph nodes

H&E and MCT4 expression are shown in a reactive lymph node and DLBCL (A). Note that MCT4 expression is lower in a reactive lymph node than in DLBCL. MCT1 expression is shown in a reactive lymph node and DLBCL (B). Note that MCT1 expression is higher in the DLBCL cancer cells. TOMM20 expression is shown in a reactive lymph node and DLBCL. Note that TOMM20 expression is higher in DLBCL cancer cells.

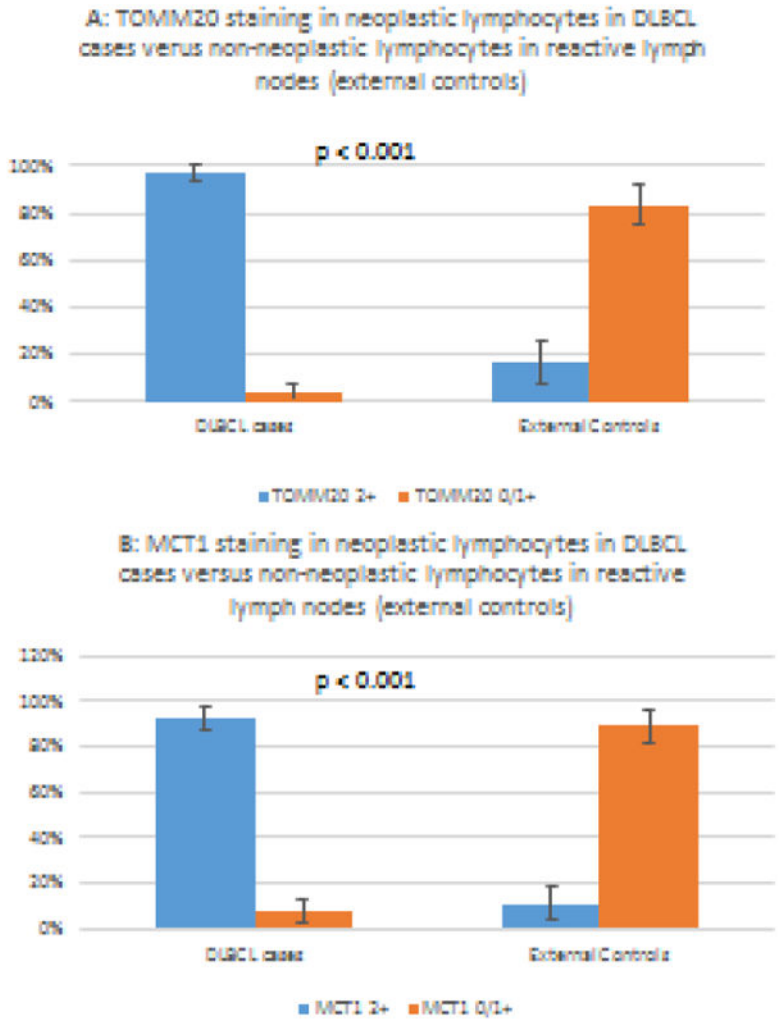

Fig 5. TOMM20 and MCT1 staining in cancer cells in DLBCL and in reactive lymphocytes in reactive lymph nodes

Note that neoplastic lymphocytes in diffuse large B-cell lymphoma stain stronger for TOMM20 than non-neoplastic lymphocytes in control lymph nodes (A). Note that neoplastic lymphocytes in diffuse large B-cell lymphoma stain stronger for MCT1 than non-neoplastic lymphocytes in control lymph nodes (B).

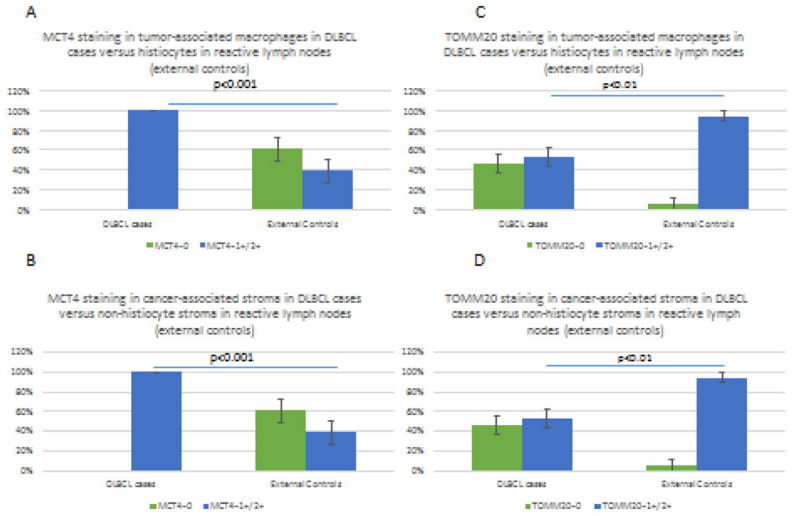

Fig 6. MCT4 and TOMM20 staining in non-cancer cells in DLBCL and in reactive lymph nodes

Note that MCT4 staining is stronger in tumor-associated macrophages (TAM) and cancer-associated stroma (CAS) in diffuse large B-cell lymphoma compared to stromal elements (macrophage and non-macrophage stroma) in non-neoplastic controls (A–B). Note that TOMM20 staining is stronger in the stroma (macrophage and non-macrophage) of non-neoplastic lymph nodes compared to tumor-associated macrophages (TAM) and cancer-associated stroma (CAS) in diffuse large B-cell lymphoma (C-D).

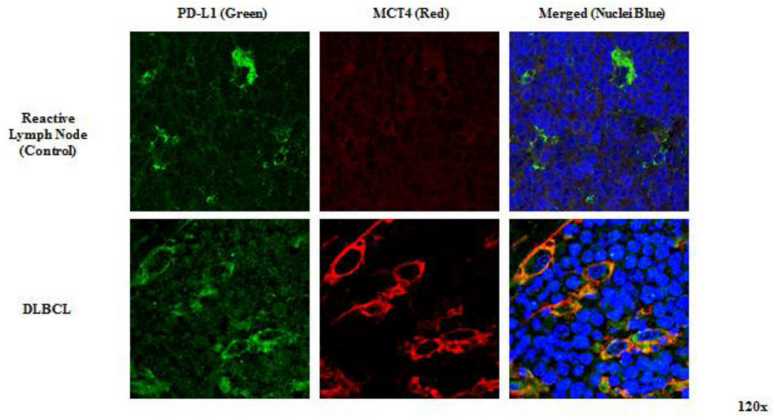

Fig 7. PD-L1 and MCT4 staining in reactive lymph node and DLBCL

Expression of PD-L1 (green) and MCT4 (red) is shown in a reactive lymph node and in diffuse large B-cell lymphoma (DLBCL). Note that there is colocalization of PD-L1 and MCT4 in DLBCL but this is absent in a reactive lymph node.

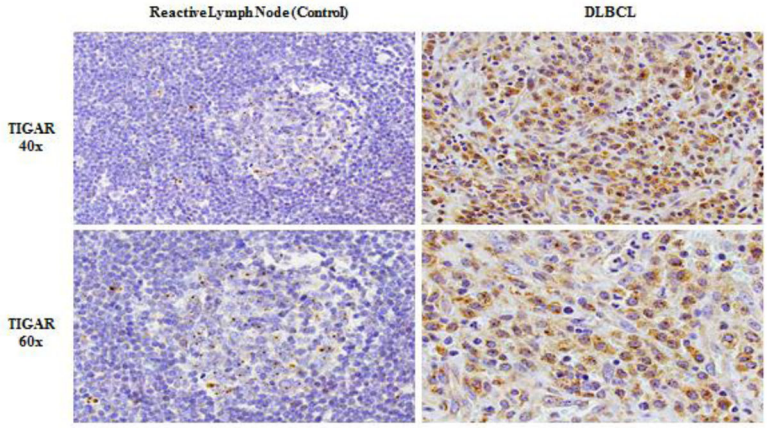

Fig 8. TIGAR staining in reactive lymph node and DLBCL

Expression of TIGAR (brown) in a reactive lymph node and in diffuse large B-cell lymphoma (DLBCL) is shown at 40x and 60x magnification. Note that there is higher TIGAR expression in DLBCL than in a reactive lymph node although it his higher in the germinal center region compared to the rest of the reactive lymph node.

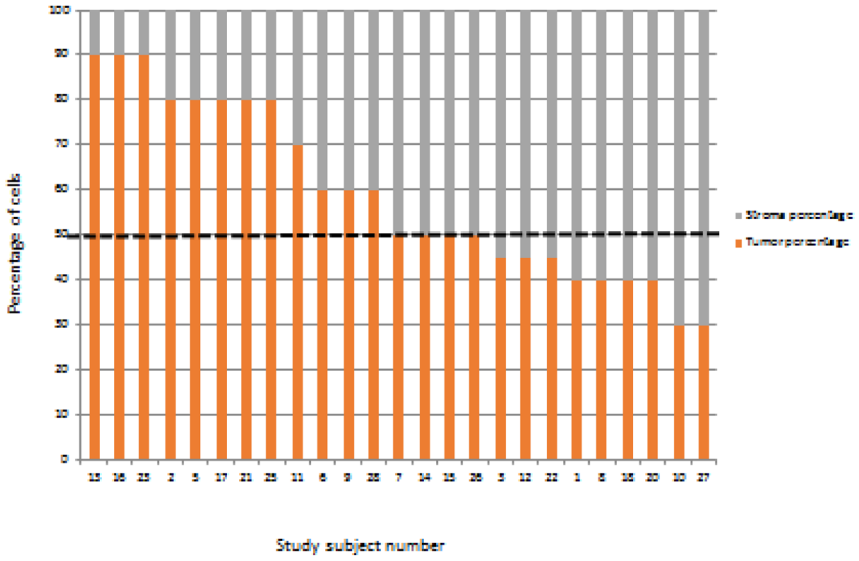

Fig 9. Percentage of Stromal and Cancer cells in DLBCL

Percentage of cancer cells (also named neoplastic lymphocytes or tumor cells (T) and stromal elements in diffuse large B-cell lymphoma cases. Note that 50% is the median percentage of cancer cells in tumors and that there is great inter-sample variability in the proportion of cancer to stromal elements.

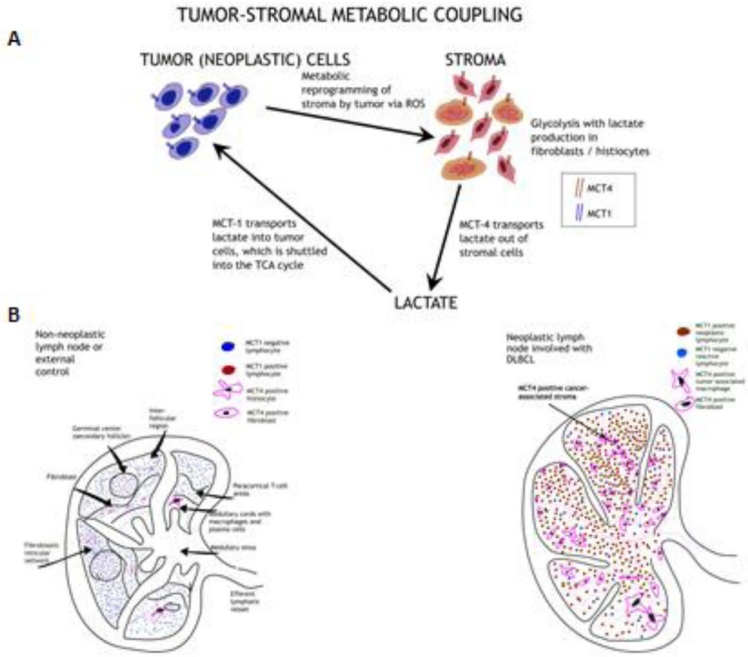

Fig 10. Model of Tumor-Stromal Metabolic Coupling in DLBCL

A model of multi-compartment tumor metabolism with neoplastic-stromal metabolic coupling via reactive oxygen species (ROS) is shown (A–B). The non-neoplastic lymph node (B-left) has preserved architecture, expresses MCT1 only in germinal center lymphocytes with scant interspersed MCT4 positive macrophages. The neoplastic lymph node (B-right) has a markedly different metabolic profile since the neoplastic lymphocytes have high expression of MCT1 and the stroma has high expression of MCT4.

Table 1

Patient characteristics of Diffuse Large B-cell Lymphoma cases (Cohort 1)

	AGE (YRS)	SEX	STAGE	R-IPI	GC/ABC	KI- 67> 70%	MAX SUV	TREATMENT	RESPONSE
1	55	M	IV	Poor	ABC	No	19.8	R-CHOP x 6, R-ICE x 2, Autologous HSCT	CR1, Relapse
2	82	F	IV	*	*	*	*	Radiation	Died prior to CR1
3	49	M	IV	Good	GC	Yes	19.0	RCHOP x 6,R-ICE x 2, Allogeneic HSCT	PR1, Relapse
4	57	M	*	*	*	*	*	RCHOP x 6 (then lost to follow-up)	CR1, Relapse
5	60	F	IV	Good	GC	Yes	3.5	RCHOP x 6	**CR1, No relapse**
6	26	M	IV	Poor	*	*	18.8	ABVD, BEACOPP (transformed from Hodgkin lymphoma)	CR1, Relapse
7	79	M	IV	Poor	ABC	No	*	RCHOP x 6,radiation to epidural mass	**CR1, No relapse**
8	77	F	IV	Poor	ABC	Yes	16.5	Not available	Not available
9	57	F	IV	*	ABC	*	42.2	R-CHOP x 6,radiation to thigh mass	CR1, Relapse
10	59	M	*	*	GC	*	*	Not available	Not available
11	67	F	IV	Good	ABC	No	*	R-CHOP x 4, radiation to epidural mass	**CR1, No relapse**
12	57	M	II	Very good	ABC	*	30.7	R-CHOP x 6	**CR1, No relapse**
13	55	F	IV	Poor	GC	*	*	R-CHOP x 1 (Died following Cycle 1)	Died prior to CR1
14	79	M	IV	Poor	ABC	No	32.0	R-CHOP x 6	Primary refractory
15	85	F	IV	*	ABC	Yes	17.3	R-Cyclophosphamide/Etoposide Vincristine	**CR1, No relapse**
16	73	M	IV	Good	GC	No	7.3	R-CHOP x 3,involved field radiation	**CR1, No relapse**
17	61	F	II	*	ABC	Yes	16.5	R-CHOP x 6	**CR1, No relapse**
18	64	M	IV	Poor	ABC	*	38.9	Not available (treated at outside institution)	CR1, Relapse
19	54	M	IV	Good	GC	Yes	31	R-CHOP x 1 (Died following Cycle 1)	Died prior to CR1
20	46	F	IV	Good	ABC	Yes	27	R-CHOP (Lost to follow- up prior to CR1)	Primary Refractory
21	73	F	IV	*	ABC	No	12.7	R-CHOP x 6	**CR1, No relapse**
22	67	F	IV	*	ABC	No	*	R-CHOP x 4,R-CEOP x 2	**CR1, No relapse**
23	63	M	IV	Poor	ABC	No	6.6	R-CHOP x 6, Autologous HSCT	CR1, Relapse
24	53	F	IV	Poor	GC	*	26.9	R-CHOP, R-ESHAP, Autologous HSCT	CR1, Relapse
25	68	F	I	*	ABC	Yes	20.8	R-CHOP x 3 ,radiation	Primary refractory
26	88	F	IV	Poor	GC	*	9.8	R-CHOP x 6	**CR1, No relapse**
27	60	M	IV	Good	GC	*	23.5	R-CHOP x 6	**CR1, No relapse**

	AGE (YRS)	SEX	STAGE	R-IPI	GC/ABC	KI- 67> 70%	MAX SUV	TREATMENT	RESPONSE
28	55	F	IV	Poor	GC	Yes	*	R-EPOCH x 2, R-ESHAP	Primary refractory

R-IPI=Revised International Prognostic Index. GC=Germinal center subtype. ABC=Activated B-cell subtype. R-CHOP=Rituximab, Cyclophosphamide, Doxorubicin, Vincristine, Prednisone. R-ICE=Rituximab, Ifosfamide, Carboplatin, Etoposide. ABVD=Doxorubicin, Bleomycin, Vinblastine, Dacarbazine. BEACOPP=Bleomycin, Etoposide, Doxorubicin, Cyclophosphamide, Vincristine, Procarbazine, Prednisone. R-CEOP=Rituximab, Cyclophosphamide, Etoposide, Vincristine, Prednisone. R-ESHAP=Rituximab, Etoposide, Solumedrol/Methylprednisolone, Cytarabine (high-dose), Cisplatin. HSCT=Hematopoietic stem-cell transplant. CR1=First Complete Remission

Table 2

Patient characteristics of patients with Double-Hit subtype of Diffuse Large B-cell Lymphoma or Cohort 2

	AGE	SEX	STAGE	R-IPI	Ki-67	TREATMENT	RESPONSE
1	61	F	IV	Poor	70%	R-EPOCH X 5,ICE X 1	**Primary refractory**
2	77	M	IV	Poor	90%	R-CHOP X 6, Rituximab maintenance	**Complete remission**
3	33	M	I	Good	100%	R-CHOP X 4,XRT	**Complete remission**
4	56	F	I	Very good	80%	R-CHOP/HD MTX X 6, Radiation	**Complete remission**
5	92	M	I	Good	80%	Surgery,XRT,Rituximab	**Partial remission**

R-IPI=Revised International Prognostic Index. R-CHOP=Rituximab, Cyclophosphamide, Doxorubicin, Vincristine, Prednisone. ICE=Ifosfamide, Carboplatin, Etoposide. XRT=radiation.

Table 3

TOMM20, MCT4 and MCT1 staining patterns in Diffuse Large B-cell Lymphoma cases or Cohort 1

S.No		TOMM20				MCT4				MCT1		
	C	CAS	TAM	RL	C	CAS	TAM	RL	C	CAS	TAM	RL
1	**2+**	1+	1+	1+	**0**	2+	2+	0	**2+**	1+	1+	1+
2	**2+**	0	0	1+	**0**	1+	2+	0	**2+**	1+	1+	1+
3	**2+**	1+	1+	1+	**0**	2+	2+	0	**2+**	1+	1+	1+
4	**2+**	1+	1+	1+	**0**	2+	2+	0	**2+**	1+	1+	1+
5	**2+**	0	0	1+	**0**	1+	2+	0	**2+**	1+	1+	1+
6	**2+**	0	0	1+	**0**	1+	2+	0	**2+**	1+	1+	1+
7	**2+**	1+	1+	1+	**0**	2+	2+	0	**2+**	1+	1+	1+
8	**2+**	1+	1+	1+	**0**	2+	2+	0	**2+**	1+	1+	1+
9	**2+**	0	0	1+	**0**	1+	2+	0	**2+**	1+	1+	1+
10	**2+**	1+	1+	1+	**0**	1+	1+	0	**2+**	0	1+	0
11	**1+**	0	0	0	**0**	1+	1+	0	**2+**	1+	1+	1+
12	**2+**	1+	1+	1+	**0**	2+	2+	0	**2+**	1+	1+	1+
13	**2+**	0	0	1+	**0**	1+	1+	0	**2+**	0	0	1+
14	**2+**	1+	1+	1+	**0**	2+	2+	0	**2+**	1+	1+	0
15	**2+**	0	0	1+	**0**	1+	2+	0	**2+**	0	0	1+
16	**2+**	0	0	1+	**0**	1+	2+	0	*****	*	*	*
17	**2+**	1+	1+	1+	**0**	2+	2+	0	**2+**	0	0	1+
18	**2+**	0	0	1+	**0**	2+	2+	0	**2+**	1+	1+	1+
19	**2+**	1+	1+	1+	**0**	1+	1+	0	**2+**	1+	1+	1+
20	**2+**	0	0	1+	**0**	1+	1+	0	**1+**	0	0	0
21	**2+**	0	0	1+	**0**	1+	2+	0	**2+**	0	0	1+
22	**2+**	1+	1+	1+	**0**	2+	2+	0	**2+**	1+	1+	1+
23	**2+**	1+	1+	1+	**0**	1+	1+	0	**2+**	1+	1+	1+
24	**2+**	1+	1+	1+	**0**	2+	2+	0	**2+**	1+	1+	1+
25	**2+**	0	0	1+	**0**	1+	1+	0	**2+**	1+	1+	1+
26	**2+**	0	0	1+	**0**	2+	2+	0	**2+**	0	0	1+

Semin Oncol. Author manuscript; available in PMC 2018 October 10.

S.No		TOMM20				MCT4				MCT1		
	C	CAS	TAM	RL	C	CAS	TAM	RL	C	CAS	TAM	RL
27	2+	1+	1+	1+	0	2+	2+	0	*	*	*	*
28	2+	1+	1+	1+	0	1+	2+	0	1+	0	2+	0

TOMM20=Translocase of Outer Mitochondrial Membrane. MCT4=Monocarboxylate Transporter 4. MCT1=Monocarboxylate Transporter 1. C=Neoplastic lymphocytes. CAS=Cancer-associated stroma. TAM=Tumor-associated macrophages. RL=Reactive Lymphocytes

Table 4

TISSUE	SCORING	TOMM20	MCT1	MCT4
DLBCL				
Tumor Cells (C)	0	0(0%)	0(0%)	28(100%)
	1+	1(4%)	2(8%)	0(0%)
	2+	27(96%)	24 (92%)	0(0%)
Cancer Stroma (CAS)	0	13(46%)	8(31%)	0(0%)
	1+	15(54%)	18(69%)	15(54%)
	2+	0	0	13(46%)
Tumor Macrophages (TAM)	0	13(46%)	6(23%)	0
	1+	15(54%)	19(73%)	7(25%)
	2+	0	1(4%)	21(75%)
mcDouble Hit DLBCL				
Tumor Cells (C)	0	0	0	5(100%)
	1+	0	0(0%)	0
	2+	5(100%)	5(100%)	0
Cancer Stroma (CAS)	0	0	5(100%)	0
	1+	5(100%)	0	5(100%)
	2+	0	0	0
Tumor Macrophages (TAM)	0	0	5(100%)	0
	1+	5(100%)	0	0
	2+	0	0	5(100%)
Non-Neoplastic Nodes				
Lymphocytes (L)	0	2(11%)	2(11%)	18(100%)
	1+	13(72%)	14(78%)	0
	2+	3(17%)	2(11%)	0
Non-macrophage stroma (NMS)	0	1 (6%)	9(50%)	11(61%)
	1+	17(94%)	8(44%)	5(28%)
	2+	0	1(6%)	2(11%)
Macrophages (M)	0	1 (6%)	9(50%)	11(61%)
	1+	17(94%)	8(44%)	5(28%)
	2+	0	1(6%)	2(11%)

Table 5

Baseline characteristics and staining patterns of patients with non-neoplastic lymph nodes (controls)

	Age	Site of biopsy	Reason for biopsy/Diagnosis	Non-neoplastic lymphocytes			Stroma (Macrophage and Non-Macrophage)		
				MCT4 MCT1		TOMM20	MCT4 MCT1		TOMM20
1	79	Neck lymph nodes (Level 2–4)	Squamous cell carcinoma larynx	0	1+	1+	1+ 1+		1+
2	77	Renal hilar lymph node	Renal cell carcinoma s/p nephrectomy	0	1+	1+	1+ 1+		1+
3	75	Pericolic lymph nodes	Ulcerative colitis s/p total proctocolectomy	0	1+	1+	0 2+		1+
4	64	Obturator lymph nodes	Prostate adenocarcinoma s/p prostatectomy	0	1+	1+	0	1+	0
5	73	Pelvic lymph nodes	Prostate adenocarcinoma s/p prostatectomy (with focal extra-prostatic invasion)	0	1+	0	0	1+	0
6	68	Lung lymph nodes (Level 1,6,11)	Sclerosing hemangioma s/p left lower lobe lobectomy	0	1+	0	2+ 1+		1+
7	52	Lung lymph nodes (Level 7,9,11,12)	Typical carcinoid tumor s/p right lower lobe lobectomy	0	1+	1+	1+	1+	0
8	36	Pericolonic lymph nodes	Chronic active colitis with fistula/adhesion s/p sigmoid colon resection	0	1+	1+	0 1+		1+
9	47	Neck lymph nodes level 2–5	Squamous cell carcinoma right hemimandible involving bone s/p hemimandibulectomy	0	1+	1+	1+ 1+		1+
10	70	Lung lymph nodes level 10	Lung adenocarcinoma s/p left upper lobe lobectomy	0	1+	1+	2+ 1+		1+
11	59	Lung lymph nodes (Level 4,7)	Lung adenocarcinoma s/p right upper lobe lobectomy with level 10 lymph nodes involved	0	0	1+	0 1+		0
12	62	Peripancreatic lymph node (station 8)	Invasive pancreatic adenocarcinoma s/p PPPD and cholecystectomy	0	1+	1+	0 1+		1+
13	40	Axillary lymph node	Lymphadenopathy- follicular and paracortical hyperplasia	0	1+	1+	0 0		1+
14	59	Axillary lymph node	Breast cancer	0	0	2+	1+ 0		1+
15	48	Axillary lymph node	Lymphadenopathy- follicular hyperplasia	0	2+	1+	0 0		1+
16	69	Neck lymph nodes (Level 2–4)	Pleomorphic salivary adenoma	0	1+	1+	0 0		1+
17	23	Right neck mass	Lymphadenopathy follicular and paracortical hyperplasia	0	2+	2+	0 0		1+

	Age	Site of biopsy	Reason for biopsy/Diagnosis	Non-neoplastic lymphocytes			Stroma (Macrophage and Non-Macrophage)		
				MCT4 MCT1		TOMM20	MCT4 MCT1		TOMM20
18	58	Right neck mass	Mild paracortical hyperplasia	0	2+	1+	0 0		1+

TOMM20=Translocase of Outer Mitochondrial Membrane. MCT4=Monocarboxylate Transporter 1. MCT4=Monocarboxylate Transporter 4